SEASONAL ACTIVITY OF GULLIES IN SOUTH POLAR PITS. J. Raack[1], D. Reiss[1], M. Vincendon[2], O. Ruesch[1], T. Appéré[3], and H. Hiesinger[1], [1]Westfälische Wilhelms-Universität, Wilhelm-Klemm-Str. 10, 48149 Münster, Germany, (jan.raack@uni-muenster.de), [2]Institut d'Astrophysique Spatiale, Université Paris Sud, 91400 Orsay, France, [3]Laboratoire AIM, CEA-Saclay, DSM/IRFU/SAp, 91191 Gif-sur-Yvette, France

Introduction: Seasonal changes of gullies in the south polar region were first reported by [1,2]. These changes were observed within the last two martian years (MY) on slopes of polar pits. The polar pits are located in Sisyphi Cavi at -72.5°S and 355°E and have a depth of up to ~1000 m. The material of the gullies appears to be fine grained with enclosed large boulders of about 5 m in diameter.

[2] presented an overview of all detected seasonal changes of gullies in the southern hemisphere (~30-70°S) without however a clear differentiation of gullies on dunes, on slopes in mid-latitudes or on slopes of polar pits. In their estimation all present activity of gullies is related and possibly shares the same forming mechanism (probably CO_2 ice related).

With high-resolution imaging, temperature and spectral data, as well as spectral modeling, we analyze the exact timing of changes to detect the possible medium (CO_2, H_2O, or dry) and the mechanism which initiate present day gully activity. In our investigations we focus only on gullies in polar pits.

Background: Seasonal activity of gullies under current climatic conditions on Mars was observed by [1-6]. These observations were made on mountain and/or crater slopes [2-4], on dune slopes at mid-latitudes [2,5,6] and on slopes of polar pits [1,2]. The suggested mechanisms to form new gully deposits are melting of H_2O ice [3,5] or sublimation/removal of CO_2 ice [2,4,6].

Recent polar gullies in the southern polar region were also analyzed by [7]. On the basis of observations made with Mars Orbiter Camera (MOC) and Thermal Emission Spectrometer (TES), gully formation was proposed to result from sublimation of CO_2 ice in spring, triggering debris avalanches [7].

Data: Our investigations are based on multiple data sets, including Context Camera (CTX) images with a resolution of ~5 m/pxl and High Resolution Imaging Science Experiment (HiRISE) images with 0.25-1 m/pxl resolution from MY 28 to 31. All images of the study region were acquired in spring and summer.

Maximum surface temperature data of the study region were derived by TES (~3 km/pxl) between ~13:00 and ~15:00 local time. With near infrared spectral data based on the Compact Reconnaissance Imaging Spectrometer for Mars (CRISM) (18 and 36 m/pxl) and on the Observatoire pour la Minéralogie, l'Eau, les Glaces et l'Activité (OMEGA) spectrometer (1.5-4.8 km/pxl) we measured the strength of the CO_2 ice absorption band (1.43 µm) and H_2O ice absorption band (1.5 µm), respectively. These band strengths are complex non linear functions of amount of volatiles, grain size/texture, and mixture type [8].

Results: *Image analysis.* Detailed analyses were made in a polar pit located in a filled crater (diameter ~54 km) north of Sisyphi Cavi at ~68.5°S and ~1.5°E. Two locations in the polar pit with clear modifications of the gullies were identified.

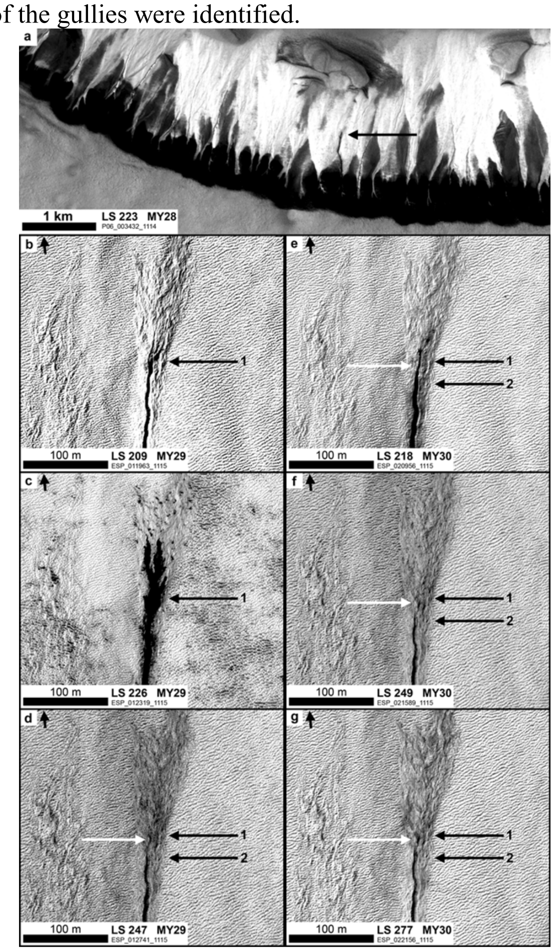

Figure 1: Sequence of seasonal behavior of the gully with morphologic changes (apron and channel termini) in spring of MY 28-30. Only one gully on the slope show a dark flow like feature (black arrow in a).

Modifications presented in this abstract can be found at 1.44°E and -68.5°S (black arrow in Fig. 1a). Dark material within the channel (Fig. 1b) leads to the formation of new dark deposits (Fig. 1c) between L_S 209° and 226° (beginning of spring) in MY 29 flowing ~70 m over the apron. The end of the gully channel is marked with a black arrow #1. At L_S 247° once ice has essentially disappeared (Fig. 2) deposition of material on the apron and within the channel shortens the channel by about 40 m (Fig. 1d; black arrow #2). The white arrow marks new deposition on the gully apron (small knob). One year later in MY 30 at L_S 218° dark material can be found within the channel, flowing ~30 m over the apron (Fig. 1e). At the end of spring (L_S 249°) the dark material faded (Fig. 1f). Retreat of the channel is not detectable. At the end of spring (Fig. 1g) no more modifications were detected.

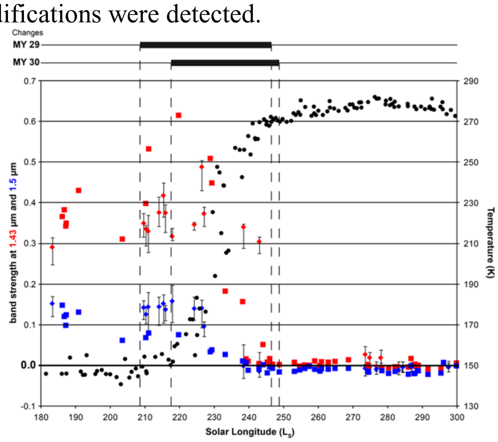

Figure 2: Measured maximum surface temperature (black dots) compared to values of CO_2 (1.43 µm) with CRISM (red diamonds) and OMEGA (red squares) and values of H_2O (1.5 µm) with CRISM (blue diamonds) and OMEGA (blue squares). First two lines represent the time range of gully changes (MY 29 and 30; dashed lines).

Temperature analysis. TES data of the area analyzed in detail (area/line at -68.5°S and from 342°E to 7°E) indicate that surface temperatures in autumn and winter are ~150 K (Fig. 2). In mid spring (L_S ~220°) temperatures increase rapidly due to solar insolation and ice sublimation. TES data show maximum surface temperatures up to ~285 K in early summer between L_S ~270° and ~310°.

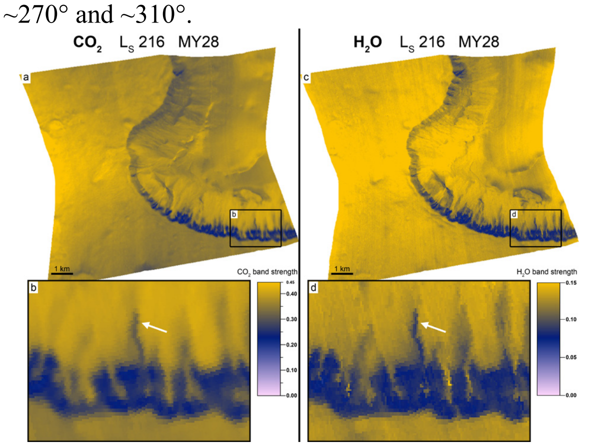

Figure 3: CRISM-image (FRT00053F5) with CO_2 band strength (a,b) and H_2O band strength (c,d). Regions with lower spectral signatures (blue regions) are found at equator-facing slopes where sun insolation reaches the maximum and where the flowing dark material is observed.

Spectral analysis. For spectral analysis we processed data from CRISM (MY 28, and 29) and OMEGA (MY 27, 28, and 29). To better understand the temporal evolution of H_2O and CO_2, the band strengths of these volatiles (ices) in all available datasets at -68.5°S in the whole study region between L_s 180° to 300° were analyzed (Fig. 2). One detailed example is shown in Fig. 3. The white arrow represent the flow within the gully channel presented in Fig. 1a. Although there are numerous gullies at the slopes of the polar pit, only the gully with the flow feature shows lowered ice band strength.

Discussion: New small deposits on the gully apron, retreat of the gully channel due to infilling, and transport of dark material within the gully channel imply seasonal (volatile) activity. The activity of the large dark flow of the gully presented here can be constrained to occur between L_S 209° (Fig. 1a) and 247° (Fig. 1c). It is not clear if the dark flow at L_S 226° (Fig. 1b) is caused by the infilling of the channel or if the material was deposited after L_S 226°.

Spectral investigations show that CO_2 and H_2O ices sublimate rapidly between L_S ~225° and ~240° (Fig. 2). This is also the time range when temperatures rises rapidly and when gully changes occurred. Detailed analyses (Fig. 3) show that ice spectral signatures are generally lower on the dark flow features. This implies either 1) a generally lower value of volatiles within gully channels due to non uniform volatile deposition on the slope, 2) a faster sublimation of volatiles within gully channels, or 3) deposition of debris above ice from the upslope regions by mass wasting.

1) The slope angle of the polar pit is very homogenous and numerous gully channels with comparable shapes and sizes can be found there (Fig. 1a). The only gully channel with lowered ice band strength (Fig. 3b,d) is the gully with the dark flow. A non uniform deposition of volatiles in only one gully channel seems implausible. 2) If the volatiles sublimate faster within gully channels we would also expect lowered ice band strengths in other gully channels on the polar pit slope, which is not the case. 3) Deposition of material by mass wasting seems to be the most plausible scenario. Our investigations show small dark spots and flows throughout the gully channel and alcove at the beginning of spring with lowered ice band strengths compared to the surroundings. This seems to be the source of material which is deposited further downslope later in mid-spring as the large dark flow (Fig. 1a,c). The temporal occurrence of gully changes (Fig. 1), temperature data (Fig. 2) and seasonal behavior of volatiles (Fig. 2,3) implies that the mass wasting is linked to, and probably caused by, defrosting of CO_2 and/or H_2O ice.

References: [1] Raack, J. et al. (2012) *LPS XXXIII*, Abstract #1801. [2] Dundas et al. (2012) *Icarus, 220,* 124-143. [3] Malin, M.C. et al. (2006) *Science, 314,* 1573-1577. [4] Dundas, C.M. et al. (2010) *GRL, 37*, doi:10.1029/2009GL041351. [5] Reiss, D. et al. (2010) *GRL, 37,* doi:10.1029/2009GL042192. [6] Diniega, S. et al. (2010) *Geology, 38,* 1047-1050. [7] Hoffman, N. (2002) *Astrobiology, 2,* 313-323. [8] Langevin et al. (2007) *JGR, 112*, E08S12.